Simple and Cooperative Electrostatic Binding of Ammonium Ions to Phosphate Polyions: NMR, Infrared, and Theoretical Study

Jaroslav Kříž* and Jiří Dybal

Institute of Macromolecular Chemistry, Academy of Sciences of the Czech Republic, Heyrovsky Sq. 2, 162 06 Prague 6, Czech Republic

Received: January 19, 2004; In Final Form: April 19, 2004

Electrostatic binding of methylammonium chloride (MAC), tetramethylammonium chloride (TMAC), and *N*-(*tert*-butoxycarbonyl)-1,6-diaminohexane hydrochloride (HAC) with phosphate glass (PG) in D_2O was studied using ^1H, ^2H, ^{14}N, and ^{23}Na NMR spectrometry, relaxometry and pulsed-field-gradient diffusion measurements, Fourier transform infrared spectroscopy, and quantum mechanical calculations. MAC, TMAC, and HAC were used as models of the functional groups of polylysine hydrochloride and its *N*-dimethyl analogue, PG (polymerization degree 45) as a polyanion with phosphate groups, a very approximate model of DNA. It was found that binding of both MAC and TMAC obeys simple laws of chemical equilibria, without any sign of cooperative behavior. In both cases, binding is slightly exothermic and entropy demanding. Its equilibrium is dynamic, with a fast exchange between bound and free ammonium cation. Inspection of ^1H NMR and in particular infrared spectra and comparison with theoretically predicted vibration frequencies shows that the bound states of MAC and TMAC are hydrated ion pairs, in which the complementary ions avoid direct contact. Nevertheless, binding of TMAC is weaker due to steric hindrances, which apparently surpass the effect of a more localized charge in this compound. In the case of HAC, binding becomes cooperative at higher concentrations and temperatures. The cause of this behavior is shown to be hydrophobic interactions of its aliphatic parts. According to ^2H quadrupolar relaxation, the driving force of this cooperativeness is the liberation of water molecules into a more disordered state.

Introduction

Electrostatic coupling of polycations with polyanions leading to ionic complexes has attracted new interest as a way to protect DNA vectors in gene manipulation and therapy. One of the leading types of such protective polycation has been poly(L-lysine) and its various derivatives.[1−9] According to our preliminary results, the binding of the polycations derived from poly(L-lysine) and its *N*-alkylated derivatives to polyphosphate anions is electrostatic and cooperative in the sense clarified in similar systems.[10−13] In contrast to general knowledge about electrostatic complexes,[14,15] according to which stronger polycations as well as polyanions offer more stable complexes, substitution of ammonium protons in poly(L-lysine) polycation by methyl groups apparently leads to less stable complexes with DNA and model polyphosphates. As the binding behavior of poly(L-lysine) polycation and its derivatives appears to be rather complicated, it is justifiable to start with a model study as the first step in its clarification. The present study deals with the electrostatic binding of methylammonium chloride (MAC), tetramethylammonium chloride (TMAC), and *N*-(*tert*-butoxycarbonyl)-1,6-diaminohexane hydrochloride (HAC) to a polyphosphate (phosphate glass, PG) in D_2O. Here, the first two substances MAC and TMAC serve as simplest possible monomeric models of the functional groups of poly(L-lysine) polycation and its *N*-trimethyl derivative, respectively. HAC is one of the substances that mimic to some degree the effect of a longer aliphatic chain attached to the functional group. The polyphosphate is of course a rather poor model of DNA but it bears phosphate anions and has the advantage of being observable by high-resolution NMR.

* Corresponding author. E-mail: kriz@imc.cas.cz. Phone: 420-296809382. Fax: 420-296809410.

Experimental Section

Materials. All chemicals were purchased in laboratory grade: methylammonium chloride (MAC) and tetramethylammonium chloride (TMAC) from Aldrich, *N*-(*tert*-butoxycarbonyl)-1,6-diaminohexane hydrochloride (HAC) from Fluka, phosphate glass PG45 (PG) from Sigma. After checking their at least 99.9% purity was checked by NMR, they were dissolved usually to a 0.01 mol/L solution in 99.9% D_2O. The mixtures were prepared by gradual adding the chloride solution to a stirred PG solution with a syringe pump. The usual addition rate was 0.5 mL/h.

NMR Measurements. ^1H, ^{23}Na, and ^{35}Cl NMR spectra, relaxations, and pulsed-field-gradient spin−echo (PGSE) measurements were obtained using a Bruker Avance DPX300 instrument with a broadband inverse-detection z-gradient probehead (used for direct measurements of proton spectra, relaxations, and part of PGSE) and broadband direct-detection probehead (^{23}Na, ^{31}P, and ^{35}Cl spectra and relaxations). Most of the methods used were described earlier.[10−13,16] ^1H PGSE or PFG-SSE (pulsed-field-gradient stimulated-echo) were done using the simple Tanner−Stejskal or Tanner sequences with 1 ms pulses of field gradients incremented in the range 15−50 G/cm and constant diffusion delay (typically 200 ms).

Infrared Measurements. Fourier transfer infrared (FTIR) spectra were measured with a Bruker IFS-55 FTIR spectrometer with a MCT detector (2048 scans per spectrum at 6 cm^{-1} resolution). Measurements were performed by an ATR technique

10.1021/jp049732u CCC: $27.50
Published on Web 05/28/2004

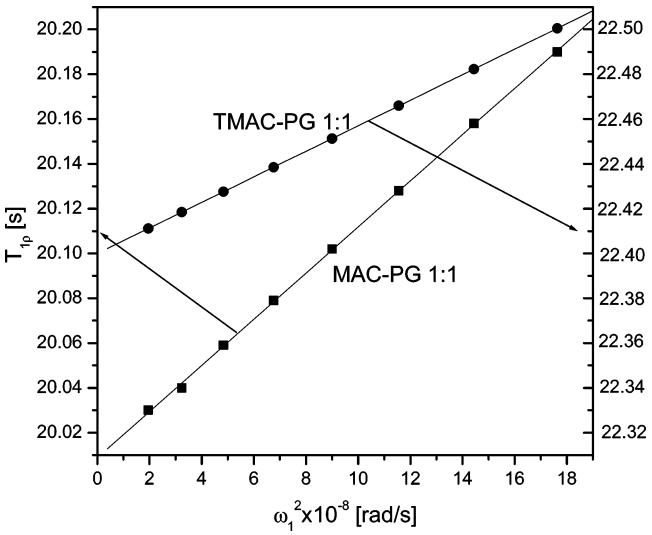

Figure 1. Dependences of $T_{1\rho}$ (±2% rel) of methyl protons on the squared spin-lock field intensity in the mixture of MAC and TMAC with PG ($\beta = 1.0$, 0.1 mol/L) at 300 K.

using the Golden Gate Heated Diamond ATR Top-Plate (Specac Ltd.) at ambient temperature.

Quantum Mechanical Calculations. Ab initio molecular orbital calculations were performed using the GAUSSIAN 98 suite of programs.[17] Geometries have been fully optimized at the B3LYP level of density functional theory (DFT) with the 6-31G+(d) and 6-311G+(2d,p) basis sets and the second-order Møller−Plesset (MP2) level of theory with the 6-31G(d) basis set.

Results and Discussion

Measured Systems and Their Characterization by ^{1}H, ^{14}N, ^{31}P, ^{23}Na, and ^{35}Cl NMR Spectra. If a PG solution is added to a stirred HAC, MAC, or TMAC solution of any concentration, the system clouds at the very first additions of PG, forming sediment in several minutes. This is, without doubt, due to the fact that the acidic solution of any ammonium chloride transforms PG into polyphosphoric acid, which is not very soluble in water. However, if HAC solution is added to PG solution, the system remains clear up to 0.9 HAC/PU (PU means a sodium phosphate unit of PG) at the concentration 20 mmol/L of both components (the concentration used below) and up to 0.4 HAC/PU at 0.1 mol/L. In the case of MAC or TMAC, the reactants can be mixed up to 1.0 MAC/PU at 0.1 mol/L (the concentration used in NMR measurements) without any clouding.

From the point of view of structural changes due to electrostatic binding, NMR spectra of any kind used here are not very informative. In ^{1}H NMR and H_2O solutions, the exchange of N−H protons with H_2O is very fast so that their signals in HAC or MAC are not visible. All further measurements were thus made in D_2O, as the exchange of N−H for N−D does not have any detectable influence on the spectrum. The rest of the ^{1}H NMR spectrum of HAC (the numbers assigned to the protons are 1−6 according to the position of methylene group, 1 being next to the ammonium group) consists of the triplets of protons 6 (3.18 ppm) and 1 (2.90 ppm), multiplets of protons 2 (2.14), 3−4 (1.81) and 5 (1.44 ppm) and a singlet of *tert*-butyl protons (1.54 ppm). The ^{1}H NMR spectrum of MAC expectedly consists of a singlet of CH_3−N protons (2.69 ppm). All other NMR spectra, i.e., ^{31}P, ^{14}N, ^{23}Na, and ^{35}Cl NMR, consist virtually (^{31}P) or entirely (^{14}N, ^{23}Na, ^{35}Cl) of one signal. ^{13}C and ^{15}N spectra could not be measured due to sensitivity but cannot be expected to offer any new information.

TABLE 1: Values Obtained for MAC and TMAC by Linear Fitting of $T_{1\rho}$ Dependence on ω_1 ($\beta = 1.0$, 300 K, D_2O, 0.1 mol/L)[a]

		MAC	TMAC	estimated error
p	(s^3/rad^2)	1.02×10^{-10}	0.57×10^{-10}	0.005×10^{-10}
q	(s/rad^2)	20.0	22.4	0.2
Δw	(rad/s)	297.4	334.1	0.6
τ_{ex}	(s)	2.3×10^{-6}	1.6×10^{-6}	0.4×10^{-6}

[a] β (mol/mol) is the molar ratio of MAC or TMAC to phosphate units.

Interaction of HAC, MAC, and TMAC with PG has little influence on the shape of any of the NMR spectra. In ^{1}H NMR, coupling to the phosphate leads to a very small downfield shift of the CH_2N triplet in HAC or the CH_3N singlet in MAC or TMAC of the order of 0.01 ppm in the 1:1 mixture of 20 mmol/L solutions. Upfield shifts due to coupling of the order of 0.1 ppm can be observed in ^{14}N (HAC, MAC, or TMAC) and ^{31}P (main signal of PG) NMR. In all cases, the shifts are linearly dependent on the coupling degree α, as shown below. As the respective signals of reactants and products are not separated, fast exchange between free and bound HAC (or MAC, TMAC) must exist. Considering the largest shifts in ^{31}P NMR, the upper bound to the exchange correlation time τ_{ex} is 10^{-2} s at most. The actual values are probably much lower, however. Probably the best method of examining fast exchange in NMR is that of measuring the rotating-frame relaxation rate in dependence on the intensity of the spin-lock field. The corresponding value of $T_{1\rho}$ then has a linear dependence on the squared spin-lock intensity ω_1 (expressed in rad/s),[18,19]

$$T_{1\rho} = \frac{4}{\Delta\omega^2\tau_{ex}} + \frac{4\tau_{ex}}{\Delta\omega^2}\omega_1^2 \qquad (1)$$

where $\Delta\omega$ is the shift between the exchanging sites. The experimental results for MAC and TMAC are given in Figure 1, and the corresponding values obtained by a linear fitting to $T_{1\rho} = q + p\omega_1^2$are shown in Table 1 (where β is the ammonium/phosphate molar ratio).

The comparison of the values of $\Delta\omega$ obtained by fitting with the actual chemical shifts suggest a low value of conversion α (fraction of phosphate units bound to MAC or TMAC), which agrees with the results given below. The values of τ_{ex} of the order of 10^{-6} s mean very fast exchange, which suggests purely electrostatic binding of MAC or TMAC to the phosphate groups without any additional interaction. As will be shown below, there are additional effects in the case of HAC at elevated temperatures.

Investigation of the Interaction Of Ammonium Salts with Phosphate Groups by FTIR and Quantum Calculations. As already explained, NMR is unable to give direct information about the details of the interaction between the ionic groups in our system due to fast exchange between N−H protons (in MAC or HAC) and water and also between the bound and free ammonium ions. The existence of such fast exchange points to the hypothesis that the interaction is purely electrostatic, however. Infrared spectroscopy is immune to the averaging effects of exchange up to correlation times $\tau_{ex} \approx 10^{-14}$ s or even less. Considering the value $\tau_{ex} \approx 10^{-6}$ s derived above, infrared spectroscopy should detect the instant states of the species in this exchange.

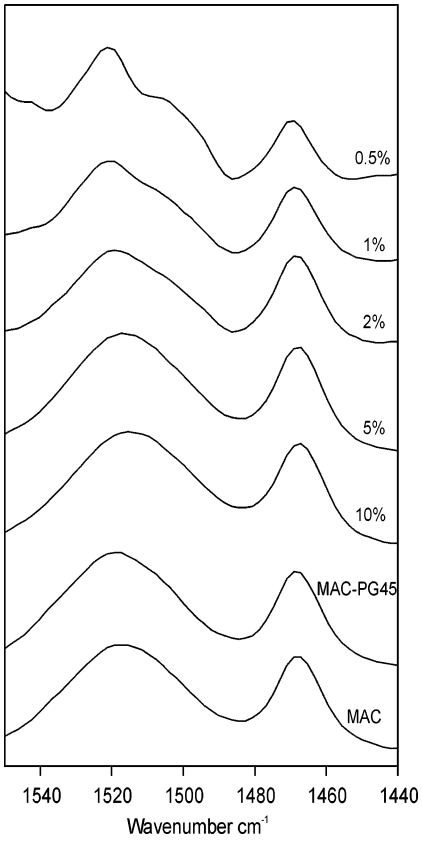

Figure 2. FTIR spectra of MAC and its mixture with PG (0.5 mol/L in H_2O at 298 K, bottom) compared with variously concentrated MAC solutions in H_2O (the indicated concentrations in % w correspond to 1.481, 0.7405, 0.296, 0.148, and 0.074 mol/L).

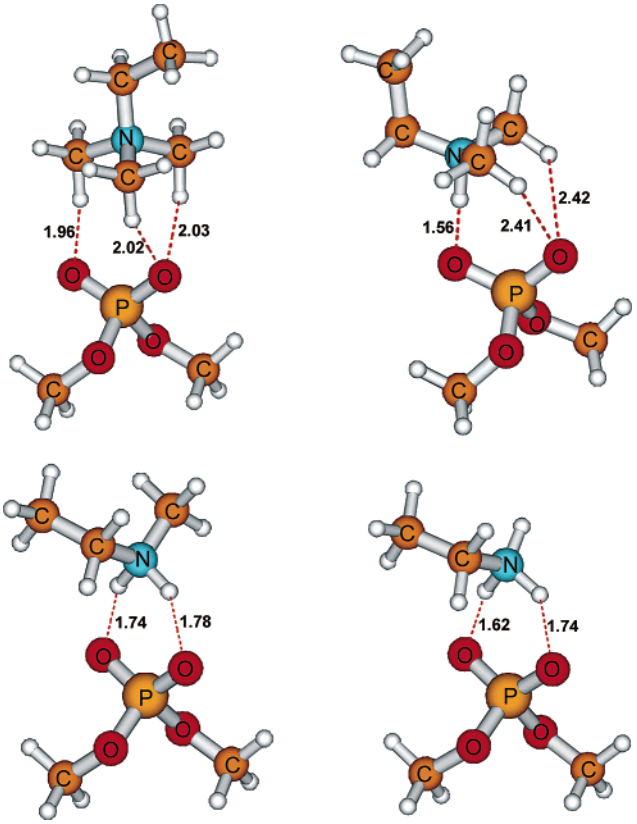

Figure 3. Optimal structures of the complexes between ethylammonium cation (down right) or its *N*-methyl, dimethyl, and trimethyl analogues and the dimethyl phosphate anion calculated at the MP2/6-31G(d) level of theory.

Figure 2 compares in the lower part the FTIR spectra (N−H and C−H deformation vibration region) of MAC in H_2O (0.5 mol/L, 298 K) with that of MAC−PG ($\beta = 1.0$). In the upper part of this figure, the development of MAC spectra with decreasing concentration in H_2O is shown. Considering first the latter part, we see that both bands with the maxima at 1468 and 1515 cm^{-1} shift with increasing dilution to higher frequency. Though the band due to the asymmetric CH_3 deformation exhibits only a small shift from 1468 to 1470 cm^{-1}, the main band due to symmetric NH_3^+ deformation vibration shifts from 1515 to 1522 cm^{-1} and narrows. At the same time, a broad shoulder appears around 1513 cm^{-1}, i.e., with its maximum slightly shifted to lower frequency compared with the main band observed at higher concentrations. On the basis of our quantum mechanical calculations (see below) and the new developments of the theory of electrolyte solutions,[20−23] we interpret this pattern as a concentration-dependent equilibrium between hydrated contact ion pairs and water-separated ion pairs.

The vibration states of both species must be affected both by primary hydration and by secondary water envelope. The first influence is evidently stronger. High-level quantum mechanical calculations reported below predict a shift of the NH_3^+ symmetric deformation vibration to higher frequency when water molecules are interleaved between the opposite ions, forming thus a water-separated ion pair. As this species cannot be much populated at high concentrations, its band starts to appear below 2% w whereas the broader band of remaining hydrated contact pairs forms a shoulder.

One can only speculate about the slight shift of this remaining band to lower frequency. Recent research on electrolyte solutions[20−22] indicates that hydrated contact ion pairs can form pseudophase areas surrounded by pure water. The size and ordering of these areas depend, among other factors, on concentration. The methods of molecular mechanics, which are able to simulate such changes, have not a sufficient precision to predict reliably the very slight changes in vibration frequencies connected with them.

At 0.5 mol/L, we should have mostly hydrated contact pairs of methylammonium and chloride ions, in which the true contact actually is somewhat eased by the hydrating water molecules. As we can see, the bands of the MAC−PG spectrum have almost exactly the same form. From this, we conclude that the bond of the methylammonium ion to the phosphate ion is purely electrostatic and has a very similar structure to that in the MAC hydrated ion pair.

As no further information can be extracted from the IR spectra, we turned to high-level quantum-mechanical calculations.

First, we compared energies of binding of ethylammonium ion and its *N*-methyl, dimethyl and trimethyl analogues to a dimethyl phosphate anion, ignoring hydration. Considering that full optimization of the structure in the DFT and especially MP2 methods is exceedingly time-consuming, we have to keep the size of the models as small as possible. Thus the ions here were chosen so that a passable similarity both to a polylysine (and its analogues) cation and DNA or RNA anion. In the cations, the aliphatic chain of the lysine unit is modeled by an ethyl group on the grounds of the knowledge that further prolonging of the aliphatic chain to propyl, butyl etc. does not change the binding properties of the ammonium group appreciably. The geometry of the optimized structures is given in Figure 3, and the binding energies are in Table 2. The binding energy was calculated as the difference of energy of fully optimized complex

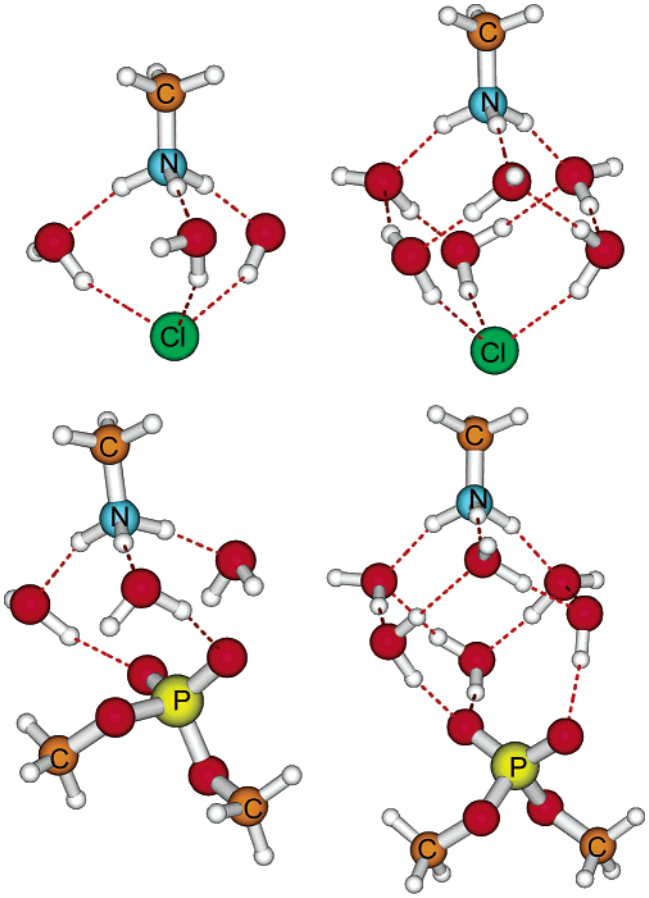

Figure 4. Optimal structures of the hydrated "contact" and water-separated ion pair of MAC and methylammonium−dimethyl phosphate calculated at the MP2/6-31G(d) level of theory.

TABLE 2: Binding Energies (kJ/mol) for Ethylammonium Cation or Its *N*-Methyl, Dimethyl, and Trimethyl Analogues with the Dimethyl Phosphate Anion Calculated by SCF-DFT and SCF-MP2 Methods

	B3LYP/6-311+G(2d,p)	MP2/6-31G(p)
$-N(CH_3)_3^+$	−378.2	−408.8
$-N(CH_3)_2H^+$	−467.8	−500.8
$-N(CH_3)H_2^+$	−486.6	−515.5
$-NH_3^+$	−507.5	−531.4

and the energies obtained for the optimized geometries of the isolated monomers.

The results of these calculations clearly show that, contrary to expectation based on simple electrostatic considerations, substitution of protons by methyl groups decreases the binding energy, making thus corresponding complexes less stable. At first glance, one could interpret this result as the effect of additional H-bonding between the less substituted ammonium ions and the oxygen atoms of the phosphate ion. Such a possibility could be indeed real in the absence of water. However, substantially different structure of the real complexes obtained in water solutions is indicated by the fact that the predicted N−H deformation vibration frequencies are quite different from those actually measured. Therefore, we simulated the structures of MAC and the corresponding phosphate complex in the presence of water molecules.

As shown in Figure 4 and Table 3, in the presence of water there are two main stable states for both chloride and phosphate types of ion pairs: (i) the hydrated contact ion pairs (with 3 water molecules) and (ii) the solvent (water)-separated ion pairs (with 6 water molecules). The hypothetically possible states with

TABLE 3: Binding Energies (kJ/mol) for Hydrated Contact and Water-Separated Ion Pairs of MAC and Methylammonium−Dimethyl Phosphate Calculated by SCF-DFT and SCF-MP2 Methods

	MP2/6-31G(d)		B3LYP/6-31+G(d)	
	I[a]	II[b]	I[a]	II[b]
MA^+_3w + Cl^-	−494.1	−735.5	−463.2	−677.0
MA^+_6w + Cl^-	−460.7	−923.4	−425.5	−825.9
MA^+_3w + DMP^-	−535.1	−776.6	−487.9	−701.7
MA^+_6w + DMP^-	−474.9	−937.2	−443.9	−843.9

[a] Binding energy calculated as the difference of energy of fully optimized complex and the energies obtained for the optimized geometries of hydrated MA^+ and corresponding anion (Cl^- or DMP^-). [b] Binding energy calculated as the difference of energy of fully optimized complex and the energies of all optimized components, i.e., MA^+, molecules of water, and anion (Cl^- or DMP^-).

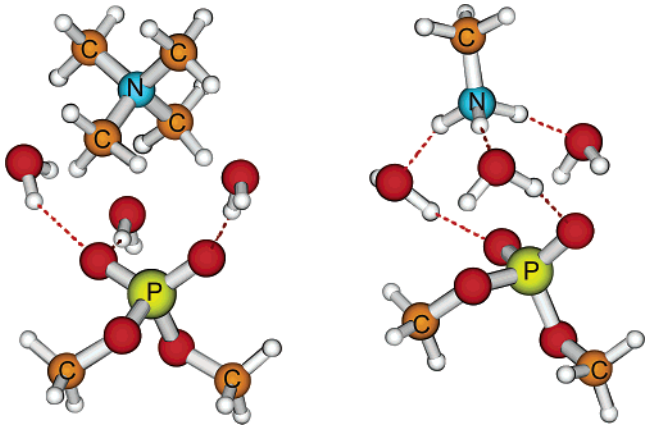

Figure 5. Optimal structures of the hydrated contact ion pairs of the tetramethylammonium ion (left) and methyammonium ion (right) with methylammonium−dimethyl phosphate calculated at the MP2/6-31G-(d) level of theory.

1, 2, 4, 5, 7, and 8 are relatively unstable. It is imaginable and indeed probable that systems of types i and ii with a much larger number of more weakly bound water molecules are possible. These are beyond the reach of high-level quantum-mechanical calculations, however.

The hydrated contact ion pair involves three water molecules in its immediate structure, which is then surrounded with further water molecules in the solution. The actual contact of opposite ions is eased by the hydrated molecules, allowing thus the symmetric NH_3^+ deformation vibration to shift to higher frequencies, compared to a true contact pair simulated above. This predicted frequency is in accord with that actually found in the experiment. In the solvent-separated ion pairs, the intertwined six water molecules increase the separation of the opposite ions, shifting thus the vibrational frequency further by 13 cm^{-1} according to the MP2 calculations (15 cm^{-1} according to DFT), which is in accord with the IR result for MAC. The results in Table 3 show that substitution of chlorine by dimethyl phosphate anion increases the binding energy.

Finally, we calculated the binding energies in the optimized structures of hydrated contact pairs of methylammonium or tetramethylammonium ions with the model phosphate anion. As shown in Figure 5, the structures are similar but not quite analogous.

The binding energies obtained with two different types of high-level calculations (second-order Møller Plesset perturbation MP2 and DFT corrections of the ab initio SCF calculation) are given in Table 4.

The results show (in accord with experimental results; see below) that, even when the contact ion pairs are eased by

TABLE 4: Binding Energies (kJ/mol) for Hydrated Contact Ion Pairs of MA^+ and TMA^+ Ions with the Dimethyl Phosphate Anion Calculated by SCF-DFT and SCF-MP2 Methods

	MP2/6-31G(d)		B3LYP/6-31+G(d)	
	I[a]	II[b]	I[a]	II[b]
TMA^+	−474.2	−636.8	−425.6	−554.4
MA^+	−535.1	−776.6	−487.9	−701.7

[a] Binding energy calculated as the difference of energy of fully optimized complex and the energies obtained for the optimized geometries of hydrated cation (TMA^+ or MA^+) and dimethyl phosphate. [b] Binding energy calculated as the difference of energy of fully optimized complex and the energies of all optimized components, i.e., cation (TMA^+ or MA^+), molecules of water, and dimethyl phosphate.

hydrating water, the binding energy for MA^+ is substantially (about 30 kcal/mol) higher than for TMA^+. The difference must be due to higher steric demands of the more bulky TMA^+ ion resulting in a somewhat large distance of the opposite charges in the ion pair.

Determination of the Coupling Degree of MAC, TMAC, or HAC to PG. The following NMR parameters perceptibly change under changing MAC/phosphate ratio β: chemical shifts of (i) ^{1}H in methyl protons, (ii) ^{13}C in methyl carbon, and (iii) ^{31}P in the main signal of PG; further longitudinal relaxation rates of (iv) ^{1}H in MAC, (v) ^{23}Na in Na^+ counterions, (vi) ^{35}Cl in Cl^- counterions, and (vii) ^{14}N in MAC; and, finally, (viii) self-diffusion coefficient of MAC measured by ^{1}H PGSE. From these, (i), (iv), and (vi) are too slight to be reliable, (ii) is unpractical due to low sensitivity. The rest, i.e., (iii), (v), (vii), and (viii), were examined.

Under conditions of fast exchange between bound and free states, the following simple relation has been shown[10−13] to be a good approximation:

$$X = \varphi X_F + (1 - \varphi)X_B \qquad (2)$$

where φ is the molar fraction of the given species in the free state and X stands for any of the following quantities: chemical shift δ, longitudinal relaxation rate R_1 (^{1}H, ^{23}Na, and ^{35}Cl in our case) and self-diffusion coefficient D. The indexes F and B refer to the free and bound state, respectively. For R_1 or D, eq 2 is a good approximation if the respective intensity decay (time dependence for R_1 and squared gradient dependence for D) is strictly monoexponential (otherwise, i.e., under conditions not fulfilling the extreme-narrowing condition, R_1 is more complicated[21]).

The well-known difficulty when applying eq 2 is that either X_F or X_B is not directly measurable and has to be obtained by extrapolation. The exception is R_1 of the counterions, where relaxation rates for both states can be obtained. Here, R_{1F} refers to the relaxation of the free ion liberated by the electrostatic coupling of its complementary ion whereas R_{1B} is the relaxation rate of the same ion in the solution of the original reactant itself. In the case where the reactant is ionized to some degree, R_{1B} does not refer strictly to a bound state of the counterion but to the dynamic equilibrium between ionized and bound states in the reactant solution. In the present case, HAC, MAC, and TMAC are strongly ionized (which does not necessarily mean strictly free ions but could correspond to strongly water-separated, rapidly exchanging ion pairs) at the concentrations used so that there is only a very small difference between R_B and R_F of ^{35}Cl anions, making thus ^{35}Cl not suitable for our purposes. Fortunately, the case of ^{23}Na ions is much more advantageous. PG as a densely charged polyion of sufficient length binds a sufficient fraction of Na^+ counterions to make a 1 order of magnitude difference between R_B and R_F, as shown for different temperatures in Figure 6.

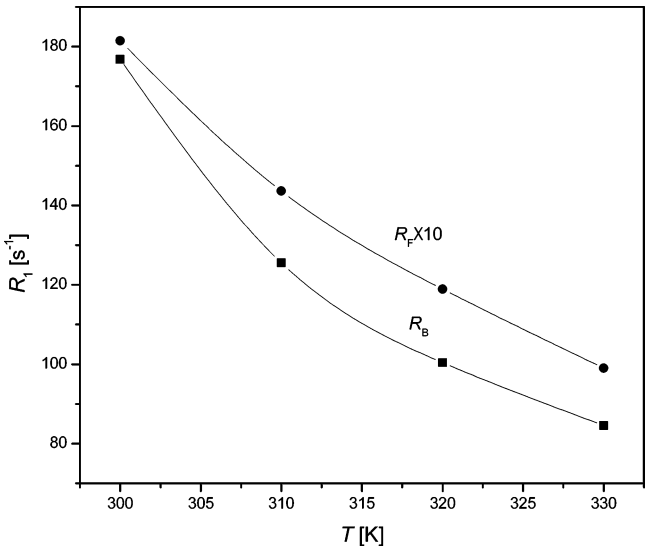

Figure 6. ^{23}Na longitudinal relaxation rates (±2% rel) in 0.01 mol/L solutions of NaCl (R_F) and PG (R_B) in D_2O at different temperatures.

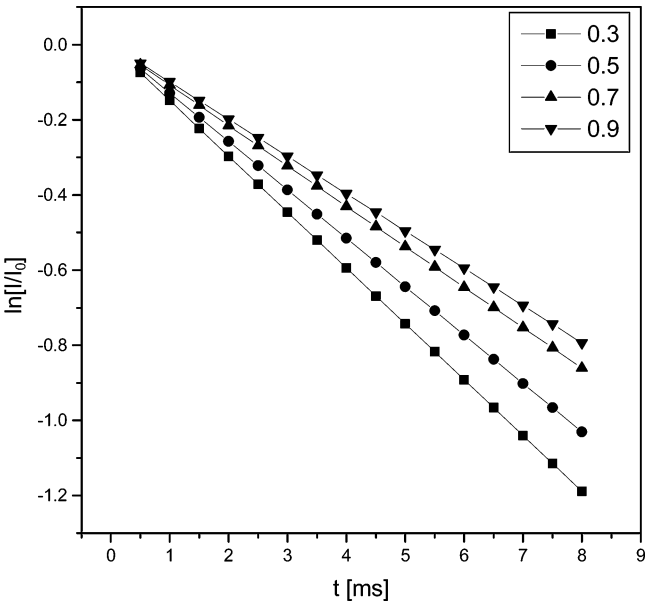

Figure 7. ^{23}Na longitudinal relaxation decays in the mixtures of PG (0.1 mol/L) with indicated equivalents of MAC at 300 K in D_2O.

Assigning φ to the molar fraction of free Na^+ ions, we thus can use eq 2 in the form

$$\varphi = \frac{R_B - R_1}{R_B - R_F} \qquad (3)$$

and the degree of MAC or HAC conversion with PG (their coupling degree) α can be obtained from φ by a simple relation

$$\alpha = \varphi/\beta \qquad (4)$$

where β is the molar ratio of MAC (or TMAC, HAC) to the PG phosphate groups.

Figure 7 shows an example of ^{23}Na longitudinal relaxation decays in MAC−PG mixtures for different values of β at 300 K. The semilogarithmic plot demonstrates a perfectly monoexponential course of the relaxation.

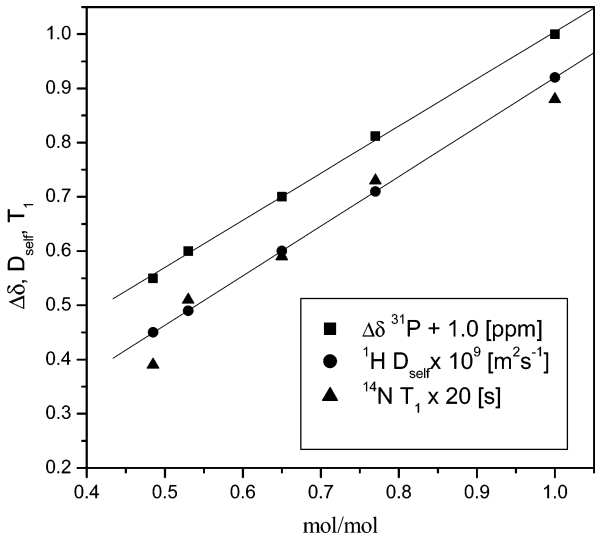

Figure 8. Correlation between the shift $\Delta\delta$ of the main ^{31}P NMR signal of PG, self-diffusion coefficient of MAC (^1H signal measure), ^{14}N longitudinal relaxation time of MAC, and the fraction of free Na ions from ^{23}Na relaxation in MAC−PG mixtures at 300 K.

If eq 2 generally holds, the chemical shift of, e.g., the main signal of PG in the mixtures, the self-diffusion coefficient of MAC and the ^{14}N relaxation time T_1 should have a linear correlation with the value of φ obtained from ^{23}Na relaxation data using eq 3. This is shown to be so for the mixtures of MAC with PG in Figure 8. Apparently, only the ^{14}N relaxation time T_1 gives poor correlation due to large experimental error. The remaining correlations give assurance that all three methods; i.e., ^{23}Na relaxation, MAC self-diffusion, and ^{31}P chemical shift, are able to offer reliable data of φ and thus the coupling degree α. However, only ^{23}Na relaxation directly gives absolute values α. Therefore, we relied on this method in the following study.

Equilibrium Binding of MAC and TMAC to PG. Let us regard now the interaction between MAC and PG as a simple equilibrium between the ammonium cation C and an independent phosphate anion A of PG on one side and their coupling product AC on the other:

$$A + C \overset{K}{\rightleftharpoons} AC \tag{5}$$

We can calculate the apparent value of K:

$$K = \frac{[AC]}{[A][C]} = \frac{\varphi}{[A]_0(1-\varphi)(\beta-\varphi)} = \frac{\alpha}{[A]_0(1-\alpha\beta)(1-\alpha)} \tag{6}$$

Figures 9 and 10 show the values of K calculated from the values of φ, obtained in the MAC−PG and TMAC−PG systems at different β and different temperatures.

Both figures show that the values K really are constant at the given temperature; i.e., eqs 5 and 6 are reasonable for these systems. In such a case, there is no surprise that the logarithmic dependences on $1/T$ are linear, as expected by the obvious eq 7 and documented in Figure 11:

$$\ln K = -\Delta H/RT + \Delta S/R \tag{7}$$

The values of ΔH and ΔS obtained from the linear fit in Figure 11 are given in Table 5.

According to the values of ΔH and ΔS, the equilibrium coupling of MAC and TMAC with PG is slightly exothermic but entropy demanding. The entropy demand is not very surprising, as the coupling restricts the dynamic states of the

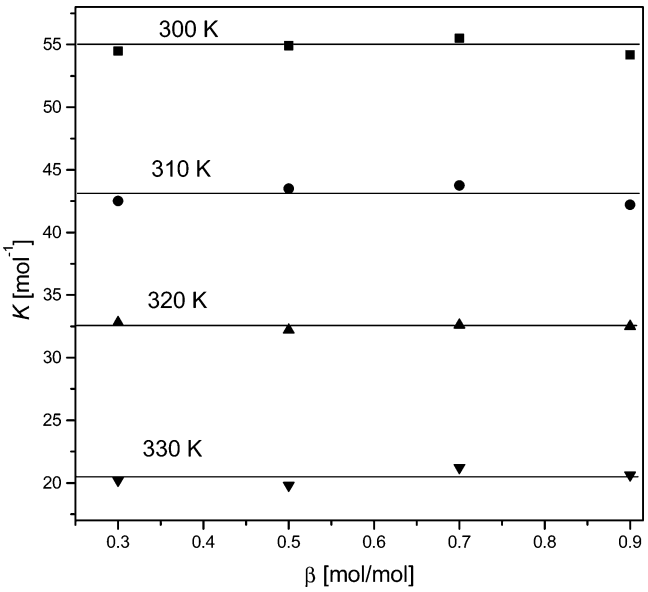

Figure 9. Values of K calculated according to eq 6 from the values of α obtained for MAC−PG systems at various β and the indicated temperatures.

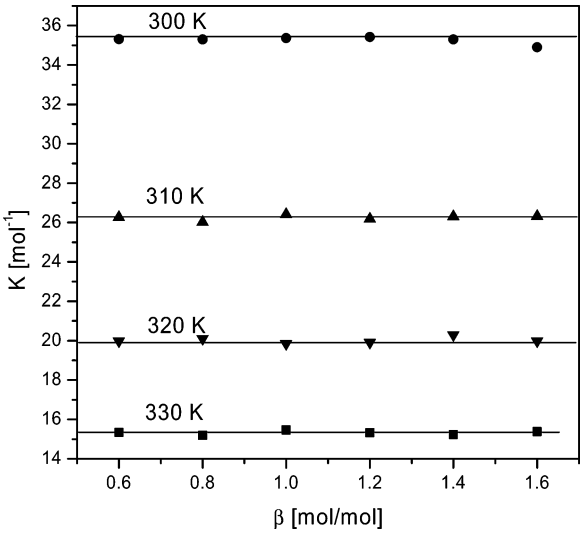

Figure 10. Values of K calculated according to eq 6 from the values of α obtained for TMAC−PG systems at various β and the indicated temperatures.

methylammonium cation. For TMAC, the values of K are generally lower and the bonding is even less exothermal than for MAC. This finding is in qualitative agreement with quantum mechanical calculations shown above (Table 3) and will be discussed below.

Equilibrium Binding of HAC to PG. A much more complicated picture, however, is offered by the coupling of HAC to the same polyphosphate. Although the same prerequisites of a reliable establishment of φ or α are fulfilled, the values of K calculated for the given β according to eq 6 are no longer equal for other β values as shown in Figure 12.

Some insight into this matter can be obtained when inspecting the dependence of α on β, as shown in two examples in Figure 13. The curves have a sigmoidal shape, which suggests cooperativity. A possible cause of the observed behavior is the hydrophobic interaction of the aliphatic chains of HAC. We already observed such interaction as a major cause of cooperativity in a complementary case of coupling of a dodecylbenzenesulfonate anion to a polycation.[13] Although the aliphatic

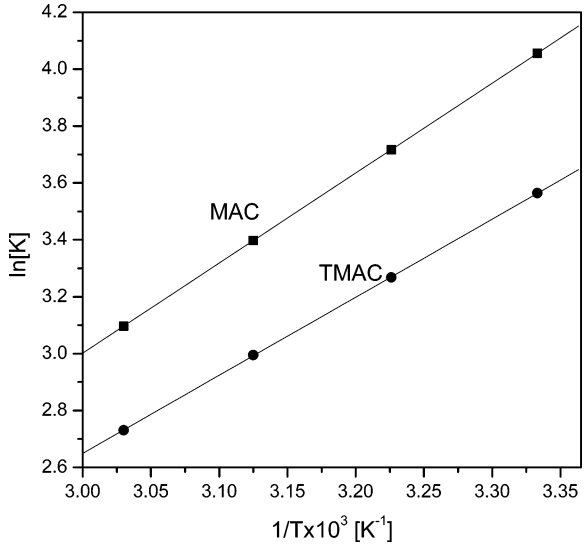

Figure 11. Correlation between ln(K) and 1/T for the systems MAC−PG and TMAC−PG ($\beta = 0.6$).

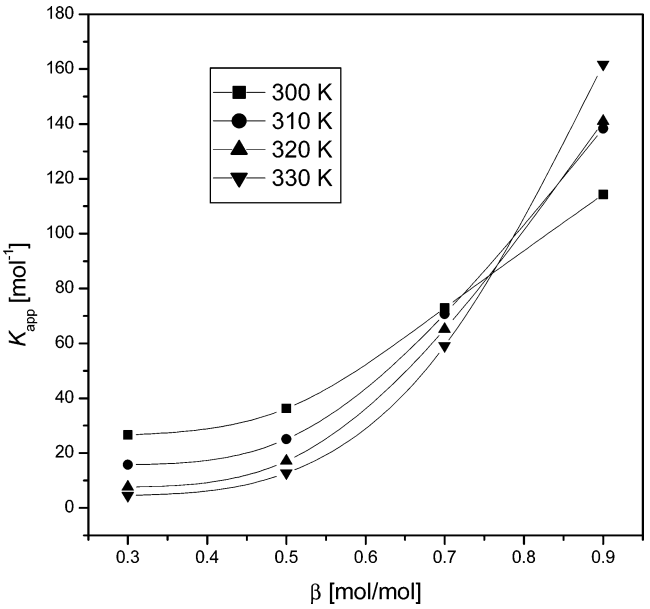

Figure 12. Apparent values of equilibrium constants K_{app} for the system HAC−PG in dependence on the ratio β at the indicated temperatures.

TABLE 5: Values of p and q in the Linear Fit ln $K_{app} = p/T + q$ and the Corresponding Apparent Values of ΔH and ΔS for the Given Values β

	MAC	TMAC	HAC				est error
β	all	all	0.3	0.5	0.7	0.9	
p	3167	2782	5957	3498	699	−1051	5
q	−6.5	−5.7	−16.5	−8.1	2.0	8.3	0.6
ΔH (kJ/mol)	−26.3	−23.1	−49.5	−29.1	−5.8	8.7	0.4
ΔS (J/mol)	−54.0	−47.4	−137.5	−67.1	16.5	68.8	0.6

chains in the latter case are substantially longer, one could speculate that the hexyl chain with a bulky *tert*-butyl group attached to it could be able to form hydrophobic domains, too.

This hypothesis is supported by the relaxation behavior of protons in the HAC chain under coupling. The transverse relaxation rate would be the most significant criterion here, but its measurement is hampered by strong scalar spin−spin coupling. Therefore, we measured rotating-frame relaxation. The intensity of the spin-lock field ω_1 was varied in a range of values low enough to approximate $T_{1\rho}$ to T_2 as much as possible.

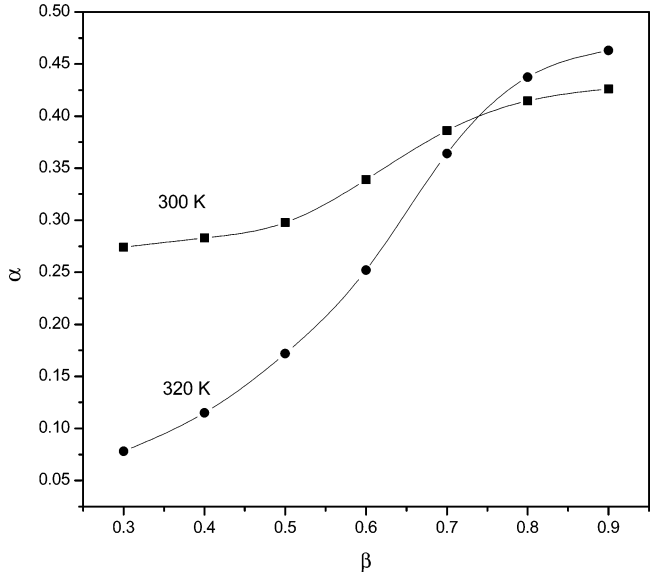

Figure 13. Dependence of the coupling degree α on β at two temperatures for the system HAC−PG.

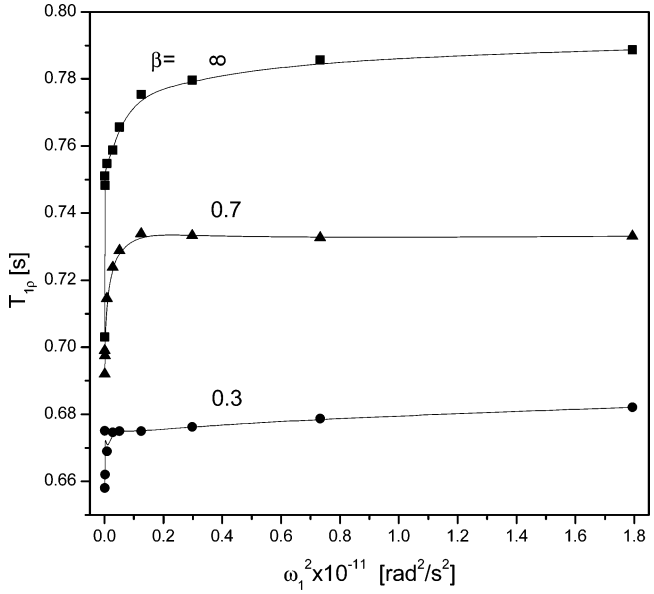

Figure 14. $T_{1\rho}$ values (±2% rel) of the ^{1}H NMR signal 1 in the solution of HAC (0.01 mol/L, $\beta = \infty$) and its mixtures with PG45 ($\beta = 0.3$ and 0.7) with dependence on the squared intensity of the spin-lock field ω_1^2 (the carrier frequency of the spin-lock field set on the signal frequency).

Figures 14 and 15 show the results for protons 1 and 6, respectively, for 300 K. In both cases, the $T_{1\rho}$ values are almost constant over a wide range of ω_1 and decay to lower and increasingly uncertain values at low ω_1 due to spin coupling. In Figure 14, the results for higher β are nearer to free HAC although the coupling degree α is somewhat larger. The reason is probably in a faster exchange between free and bound HAC at lower β, as indicated by a higher slope of the dependence (cf. eq 1).

In Figure 15, the relation is quite the opposite: the relaxation time for $\beta = 0.7$ is now lower than that for $\beta = 0.3$. As there is no shift of signal 6 connected with HAC coupling (and thus no contribution of exchange to relaxation), the lower value of $T_{1\rho}$ in the former case should be a sign of a lower mobility of the corresponding group in the bound state, probably due to the formation of hydrophobic domains.

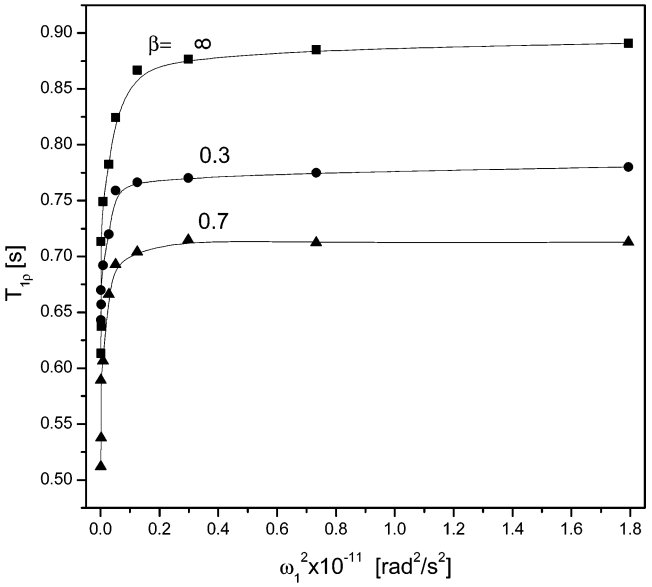

Figure 15. Same as in Figure 14 for signal 6.

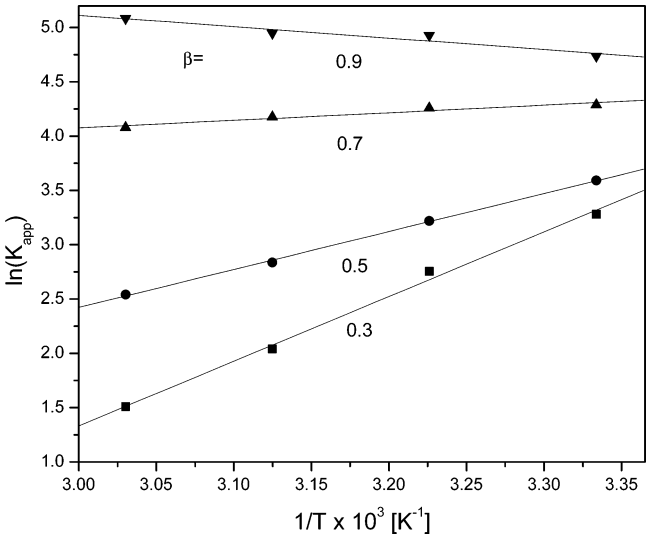

Figure 16. Temperature dependence of the apparent constants K_{app} for the system HAC−PG at indicated values of β.

As already mentioned, hydrophobic interaction has already been observed to be a driving force of cooperative coupling in the interaction of dodecylbenzenesulfonate to a polycation.[13] According to the theoretical model proposed by Kuhn−Levin−Barbosa,[24] the effect was interpreted in terms of energy rather than entropy. However, the increasing bulk of evidence[25−29] shows that hydrophobic interaction is mainly an effect of entropy gained by water molecules due to their liberation from hydrophobic hydration or simply to the increase in their partial free volume. In this connection, there is some interest in following the temperature dependence of the apparent equilibrium constants calculated for individual values of β. This is shown in Figure 16. It is immediately clear that the values of K are only apparent, as they are not constant at varied β, and so are the obtained values of ΔH and ΔS. Nonetheless, they have some heuristic value. We can see that at low values of β, the interaction behaves like an exothermal reaction with negative entropy change. This can be understood because the interaction offers a gain in electrostatic potential energy (hence the exothermal reaction) and, at the same time, it brings about a relative restriction in the possible positions of HAC (hence the loss of entropy). At higher β (and thus higher α as well), there

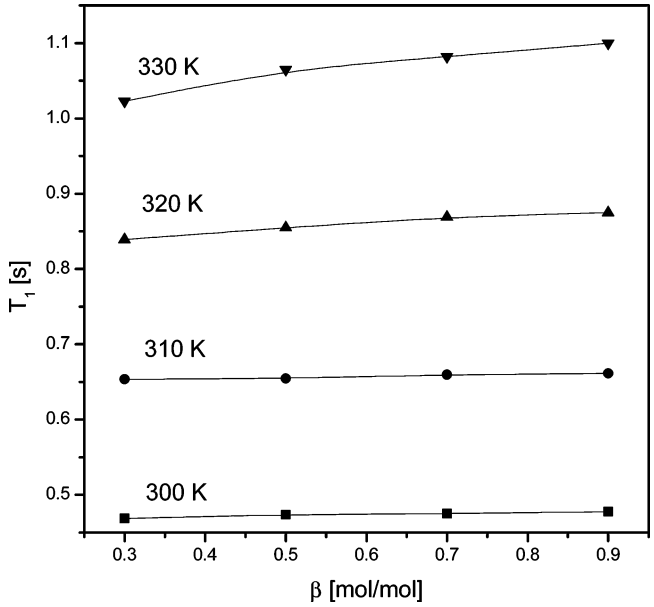

Figure 17. ^{2}H NMR relaxation times (±2% rel) of D_2O signal in systems HAC−PG with dependence on β under the indicated temperatures.

is cooperative behavior apparently driven by entropy rather than enthalpy change. This cannot be due to the states of HAC itself, which should lose entropy by bonding to PG. Higher entropy must be acquired by water molecules, as it is commonly supposed for hydrophobic interaction.[25−29]

A strong indication of the mobility states of water molecules can be obtained from the longitudinal ^{2}H NMR relaxation in the systems under inspection. This type of relaxation mostly reflects rotational diffusion states of the D_2O molecule, the usual course of decay being[30]

$$\langle I_z(t)\rangle = \langle I_z(0)\rangle \exp(-R_1 t) \tag{8}$$

where

$$R_1 = (1/T_1) = \frac{1}{10}(1+\varsigma^2/3)\left(\frac{e^2qQ}{h}\right)^2 \frac{\tau_c}{[1+(\omega\tau_c)^2]} \cong \chi_Q \tau_c \tag{9}$$

Here, ζ is the asymmetry factor, eq the electric field gradient, eQ the quadrupole moment, and χ_Q the quadrupole coupling constant and the approximation at the right side of eq 9 corresponds to the extreme narrowing limit, which is certainly fulfilled in our case. The increase in R_1 with dissolution of some relatively hydrophobic substance in water can be expected to be due to an increase in the rotational correlation time τ_c of a fraction of D_2O molecules in the solvation sphere. As the exchange between the molecules in this sphere and those in bulk water is at least 10 orders of magnitude faster than the relaxation, we get a strictly monoexponential decay according to eq 2 with X substituted for R_1. In Figure 17, the dependence of $T_1 = 1/R_1$ on β is shown for different temperatures. The increase in T_1 with increasing temperature is natural as τ_c has the approximate dependence

$$\tau_c = 4\pi R^3 \eta/(3kT) \tag{10}$$

where R is the radius of the rotational profile of the molecule and η is viscosity (decreasing with T). Much more remarkably, T_1 also increases with increasing β, the dependence being more pronounced with increasing temperature. This dependence can

only mean that a lower fraction of water molecules is hindered in their rotational motion under conditions where we cooperative coupling, i.e., that the cooperativity is connected with liberation of water from hydration sites. Such a process, of course, is connected with an increase of entropy.

Conclusions

In this study, we have shown that both methylammonium (provided by methylammonium chloride, MAC) and tetramethylammonium (from tetramethylammonium chloride, TMAC) ions bind to the polyanion of a polyphosphate in a simple equilibrium. The binding, which is in fact a substitution of sodium counterions of the polyphosphate, is slightly exothermic and rather weak so that fast exchange between bound and free ammonium ion with a correlation time $\tau_{ex} \approx 10^{-6}$ s can be detected by NMR. Using a combination of FTIR spectra and high-level quantum-mechanical calculations, we propose that the binding product in both cases (as well as MAC or TMAC at higher concentrations) has the nature of hydrated contact ion pair, in which three immediately bound water molecules increase the distance between oppositely charged ions and thus decrease the energy of electrostatic binding. There is a difference in binding energy in favor of MAC, found by both quantum mechanical calculations and NMR. According to our results, this difference is due to larger steric demands of the more bulky tetramethylammonium ion, which increase the distance between oppositely charged ions in the binding product, rather than to any other type of interaction (such as N−H···O bonding, which could favor MAC over TMAC).

We have examined five different ways of experimentally establishing the coupling degree α of MAC to a polyphosphate by NMR: (i) ^{23}Na relaxation rate of the Na^+ counterions; (ii) ^{35}Cl relaxation rate of Cl^- counterions; (iii) ^{14}N relaxation rate of the ammonium ion; (iv) ^{1}H PFG measurement of MAC self-diffusion; (v) ^{31}P chemical shift of the phosphate. Among these, (i) was found to be most reliable and unambiguous and thus used for measuring α in the examined systems.

For neither MAC nor TMAC was there found any sign of cooperative behavior in their binding to the polyphosphate. In a sharp contrast to that, binding of *N*-(*tert*-butoxycarbonyl)-1,6-diaminohexane hydrochloride (HAC) exhibits strong deviation from a simple equilibrium, in particular at higher cation/anion ratios and at higher temperatures. This deviation clearly can be interpreted as cooperative binding. Considering the experimentally found decrease of local mobility in the aliphatic part of bound HAC as well as a slight increase in rotational mobility of water in the solutions of binding products, we find as justified the hypothesis that this cooperative binding is due to hydrophobic interaction of the aliphatic parts of HAC, in particular its $(CH_2)_6$ chains.

Acknowledgment. We thank the Grant Agency of the Academy of Sciences of the Czech Republic for financial support given under the grant A4050206 and the Academy of Sciences of the Czech Republic for additional support (Projects No.: AVOZ4050913 and KSK4050111). They also thank Mrs. D. Kaňková for technical assistance.

References and Notes

(1) Maestre, M. F.; Reich, C. *Biochemistry* **1980**, *19*, 5214.
(2) Curiel, D. T.; Wagner, E.; Cotten, M.; Brirnstiel, M. L.; Agarwal, S.; Li, C. M.; Hu, P. C. *Human Gene Therapy* **1992**, *3*, 147.
(3) Erbacher, P.; Roche, A. C.; Monsigny, M.; Midoux, P. *Bioconjugate Chem.* **1995**, *6*, 401.
(4) Mamounas, M.; Leavitt, M.; Yu, M.; Wongstaal, F. *Gene Therapy* **1995**, *2*, 429.
(5) Midoux, P.; Monsigny, M. *Bioconjugate Chem.* **1999**, *10*, 406.
(6) Oupický, D.; Koňák, C.; Ulbrich, K. *Mater. Sci. Eng. C—Biomimetic Supramol. Syst.* **1999**, *7*, 59.
(7) Oupický, D.; Koňák, C.; Ulbrich, K.; Wolfert, M. A.; Seymour, L. W. *J. Controlled Release* **2000**, *65*, 149.
(8) Reschel, T.; Koňák, C.; Oupický, D.; Seymour, L. W.; Ulbrich, K. *J. Controlled Release* **2002**, *81*, 201.
(9) Oupický, D.; Reschel, T.; Koňák, C.; Oupická, L. *Macromolecules* **2003**, *36*, 6863.
(10) Kříž, J.; Kurková, D.; Dybal, J.; Oupický, D. *J. Phys. Chem. A* **2000**, *104*, 10972.
(11) Kříž, J.; Dautzenberg, H. *J. Phys. Chem. A* **2001**, *105*, 3846.
(12) Kříž, J.; Dybal, J.; Dautzenberg, H. *J. Phys. Chem. A* **2001**, *105*, 7486.
(13) Kříž, J.; Dybal, J.; Kurková, D. *J. Phys. Chem. B* **2002**, *106*, 2175.
(14) Kabanov, V. A. In *Macromolecular Complexes in Chemistry and Biology*; Dubin, P., Bock, J., Davies, R. M., Schulz, D. N., Thies, C., Eds.; Springer-Verlag: Berlin, 1994; Vol. 10, p 151.
(15) Dautzenberg, H.; Koetz, J.; Linow, K. J.; Philipp, B.; Rother, C. In *Macromolecular Complexes in Chemistry and Biology*; Dubin, P., Bock, J., Davies, R. M., Schulz, D. N., Thies, C., Eds.; Springer-Verlag: Berlin, 1994; Vol. 8, p 119(3). Philipp, B.; Dautzenberg, H.; Linow, K. J.; Koetz, J.; Dawydoff, W. *Prog. Polym. Sci.* **1989**, *14*, 91.
(16) Kříž, J.; Dybal, J.; Kurková, D. *J. Phys. Chem. A* **2002**, *106*, 7971.
(17) Frisch, M. J.; Trucks, G. W.; Schlegel, H. B.; Scuseria, G. E.; Robb, M. A.; Cheeseman, J. R.; Zakrzewski, V. G.; Montgomery, J. A., Jr.; Stratmann, R. E.; Burant, J. C.; Dapprich, S.; Millam, J. M.; Daniels, A. D.; Kudin, K. N.; Strain, M. C.; Farkas, O.; Tomasi, J.; Barone, V.; Cossi, M.; Cammi, R.; Mennucci, B.; Pomelli, C.; Adamo, C.; Clifford, S.; Ochterski, J.; Petersson, G. A.; Ayala, P. Y.; Cui, Q.; Morokuma, K.; Malick, D. K.; Rabuck, A. D.; Raghavachari, K.; Foresman, J. B.; Cioslowski, J.; Ortiz, J. V.; Baboul, A. G.; Stefanov, B. B.; Liu, G.; Liashenko, A.; Piskorz, P.; Komaromi, I.; Gomperts, R.; Martin, R. L.; Fox, D. J.; Keith, T.; Al-Laham, M. A.; Peng, C. Y.; Nanayakkara, A.; Challacombe, M.; Gill, B.; Johnson, P. M. W.; Chen, W.; Wong, M. W.; Andres, J. L.; Gonzalez, C.; Head-Gordon, M.; Replogle, E. S.; Pople, J. A. *Gaussian 98*, revision A.9; Gaussian, Inc.: Pittsburgh, PA, 1998.
(18) Deverel, C.; Morgan, R. E.; Strange, J. H. *Mol. Phys.* **1970**, *18*, 553.
(19) Ohuchi, M.; Fujito, T.; Imanari, M. *J. Magn. Reson.* **1979**, *35*, 415.
(20) Smith, E. D.; Dang, L. X. *J. Chem. Phys.* **1994**, *100*, 3757.
(21) Mizoguchi, A.; Ohshima, Y.; Endo Y *J. Am. Chem. Soc.* **2003**, *125*, 1716.
(22) Dillon, S. R.; Dougherty, R. C. *J. Phys. Chem. A* **2003**, *107*, 10217.
(23) Bull, T. E. *J. Magn. Reson.* **1872**, *8*, 344.
(24) Kuhn, P. S.; Levin, Y.; Barbosa, M. C. *Chem. Phys. Lett.* **1998**, *298*, 51.
(25) Söderman, O.; Stilbs, P. *Prog. NMR Spectrosc.* **1992**, *26*, 445.
(26) Goddard, E. D. In *Interactions of Surfactants with Polymers and Proteins*; Goddard, E. D., Ananthapadmanabhan, K. P., Eds.; CRC Press: Boca Raton, Ann Arbor, London, and Tokyo, 1992.
(27) Rick, S. W.; Berne, B. J. *J. Phys. Chem. B* **1997**, *101*, 10488.
(28) Berne, B. J. *Proc. Natl. Acad. Sci. U.S.A.* **1996**, *93*, 8800.
(29) Hummer, G.; Garde, S.; Garcia, A. E.; Pohorille, A.; Pratt, L. R. *Proc. Natl. Acad. Sci. U.S.A.* **1996**, *93*, 8951.
(30) Hubbard, P. S. *J. Chem. Phys.* **1970**, *53*, 985.